Supplementary Figure Captions

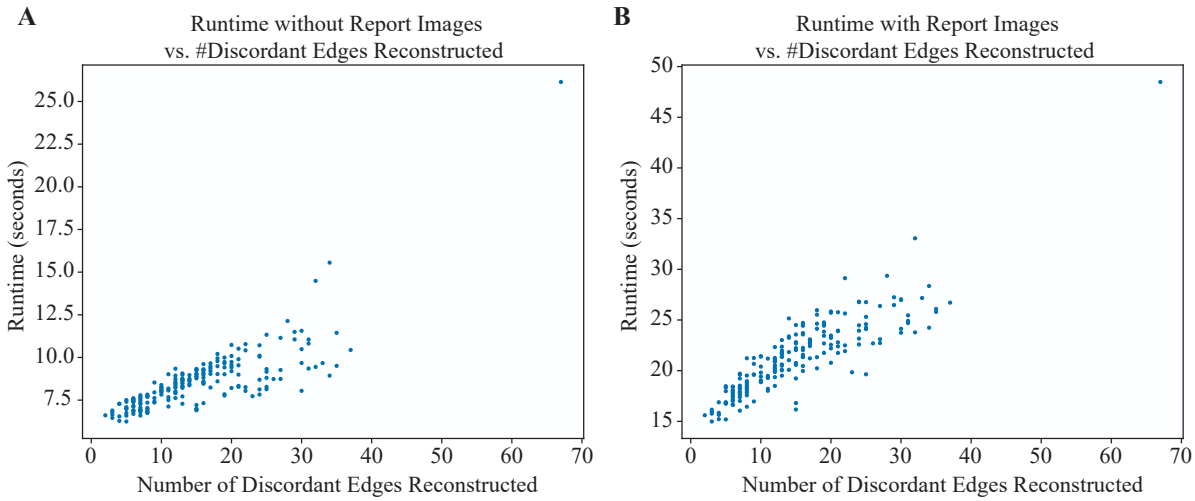

Supplementary Figure S1: **Runtime analysis**. Runtime of OMKar was collected on both simulation and clinical samples A) without rendering the visualization images in HTML report, and B) with rendering the report images.

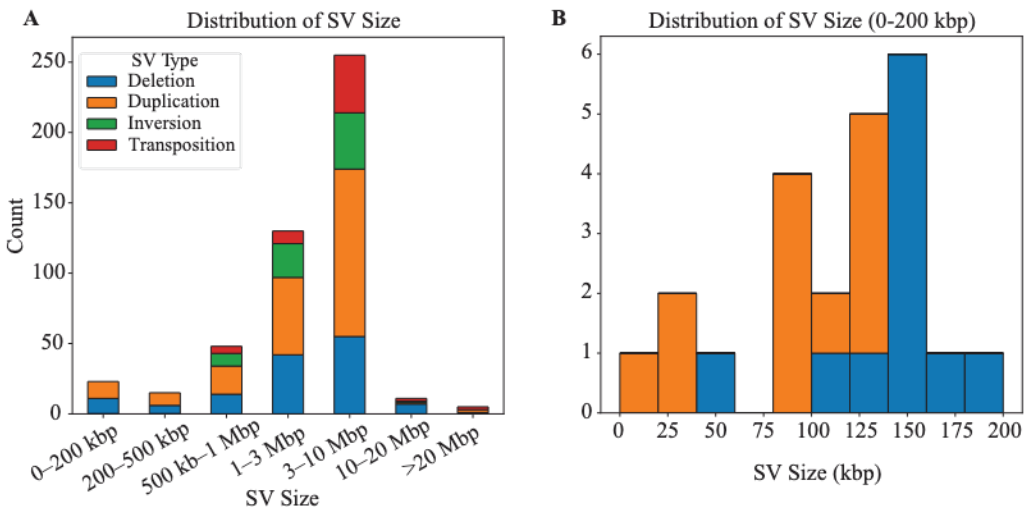

Supplementary Figure S2: **SV size distribution**. A) Binned SV size distribution of all samples evalulated. B) Detailed size distribution between 0 and 200 kbp.

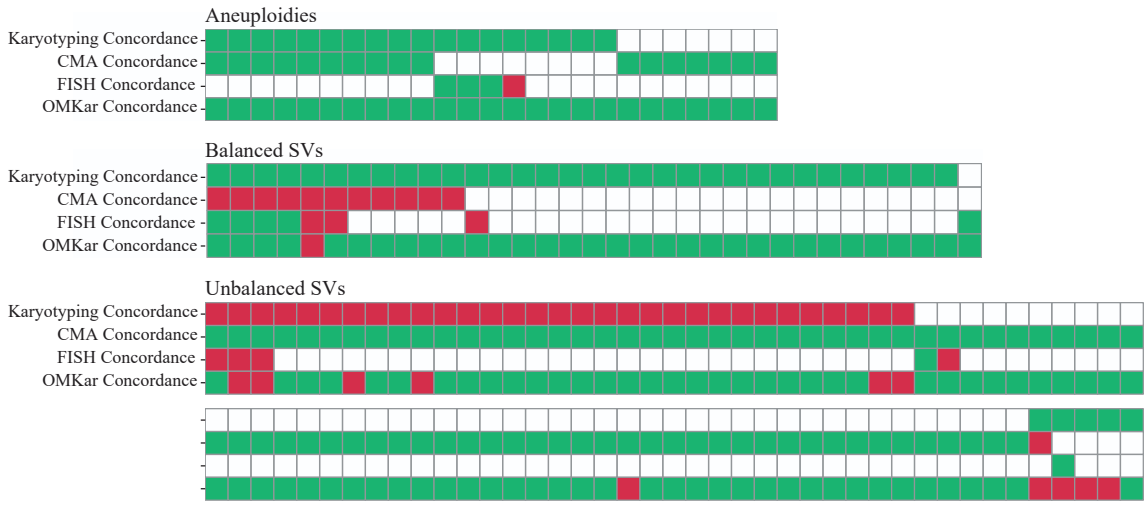

Supplementary Figure S3: **Validation of OMKar reconstruction against clinical annotation by cytogeneticists using karyotyping, CMA, and/or FISH**. OGM and OMKar was applied to all samples, but not all technology was applied on all samples. Each column represents a clinical sample. The color code in the cells explain the concordance of the applied technology. White: the technology was not applied; Green: concordance; Red: Missed. Variations were grouped into A) aneuploidies, B) balanced structural variations, and C) unbalanced structural variations. Note, the unbalanced structural variations take up two sets of rows.

A

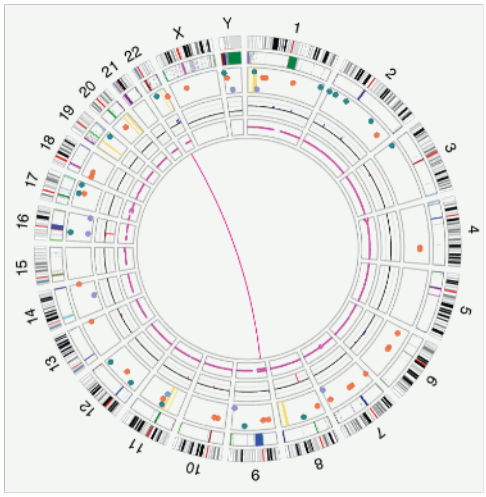

Inter-Chr Contig (1)

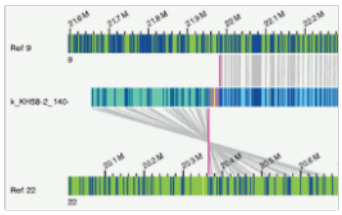

Inter-Chr Contig (2)

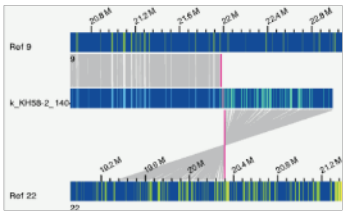

Intra-Chr Contig (3)

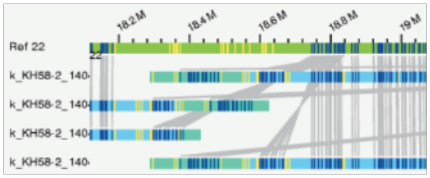

B

OMKar Karyotype

[30+, 31+, 32+, 33+]

[77-, 31+, 32+, 33+]

[72+, 73+, 74+, 75+, 76+, 77+]

[72+, 73+, 74+, 75-, 75+, 76+, 30-]

Segment	chr	start	end	size
33	Chr9	45,518,559	138,334,464	92,815,906
72	Chr22	10,514,804	12,954,788	2,439,985
73	Chr22	12,954,789	15,054,318	2,099,530
74	Chr22	15,054,319	18,764,313	3,709,995
75	Chr22	18,764,314	19,008,959	244,646

C

Clustered SVs

1. t(9;22)(p24.3;q11.21)
2. left-dup-inv(22)(q11.21)

D

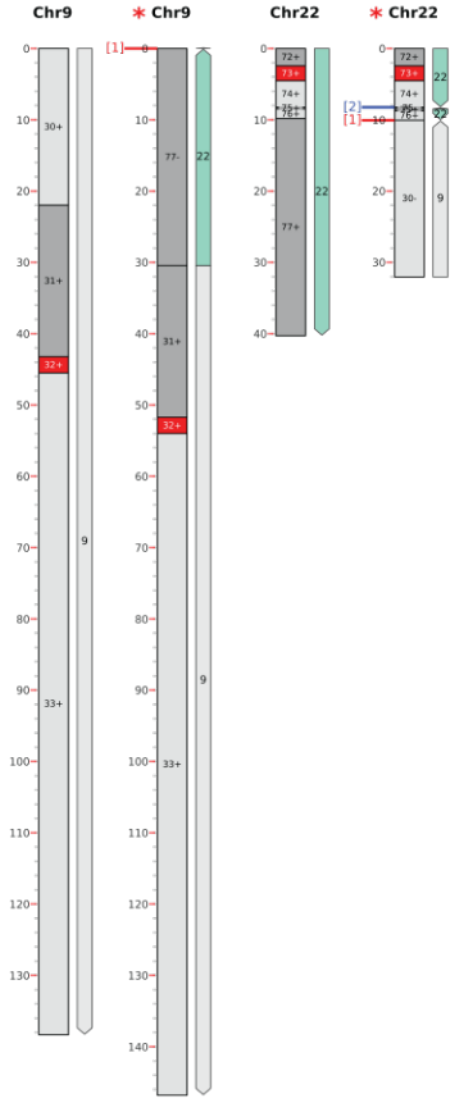

E

WT Chr9 [30+, 31+, 32+, 33+]

WT Chr22 [72+, 73+, 74+, 75+, 76+, 77+]

der Chr9 [77-, 31+, 32+, 33+]

der Chr22 [72+, 73+, 74+, 75-, 75+, 76+, 30-]

Supplementary Figure S4 (caption on next page)

Supplementary Figure S4: Supplementary Figure S4: Comparison of Bionano Access and OMKar Outputs Postnatal 1404). Postnatal sample 1404 contains a balanced reciprocal translocation between Chromosomes 9 and 22, as well as a 240 kbp left-duplication inversion on Chromosome 22, located approximately 1.3 Mbp upstream of the translocation breakpoint. (A) The inter-chromosomal translocation is called and shown on the Circos plot from Bionano Access. The two translocation contigs of the same orientation are shown on the right, alongside the contigs supporting the duplication inversion call. (B) The OMKar output on the same data gives a clear description of the karyotype as a sequence of chromosomal segments (e.g., ...74+ 75- 75+ 76+ 30-, in derivative Chromosome 22), where each segment number corresponds to a distinct genomic interval. (C) A chromosomal annotation of the OMKar reconstruction shows the canonical balanced translocation event, forming the derivative Chromosomes 9 and 22. In addition, there is a left duplication inversion on derivative Chromosome 22 upstream of the translocation. (D) As part of the automated OMKar report, the clustered SVs are also shown in ISCN format. (E) The automated chromosomal ideogram corresponding to the reconstruction is included on the right, with the chromosomal segments and the location of the clustered SV labeled.

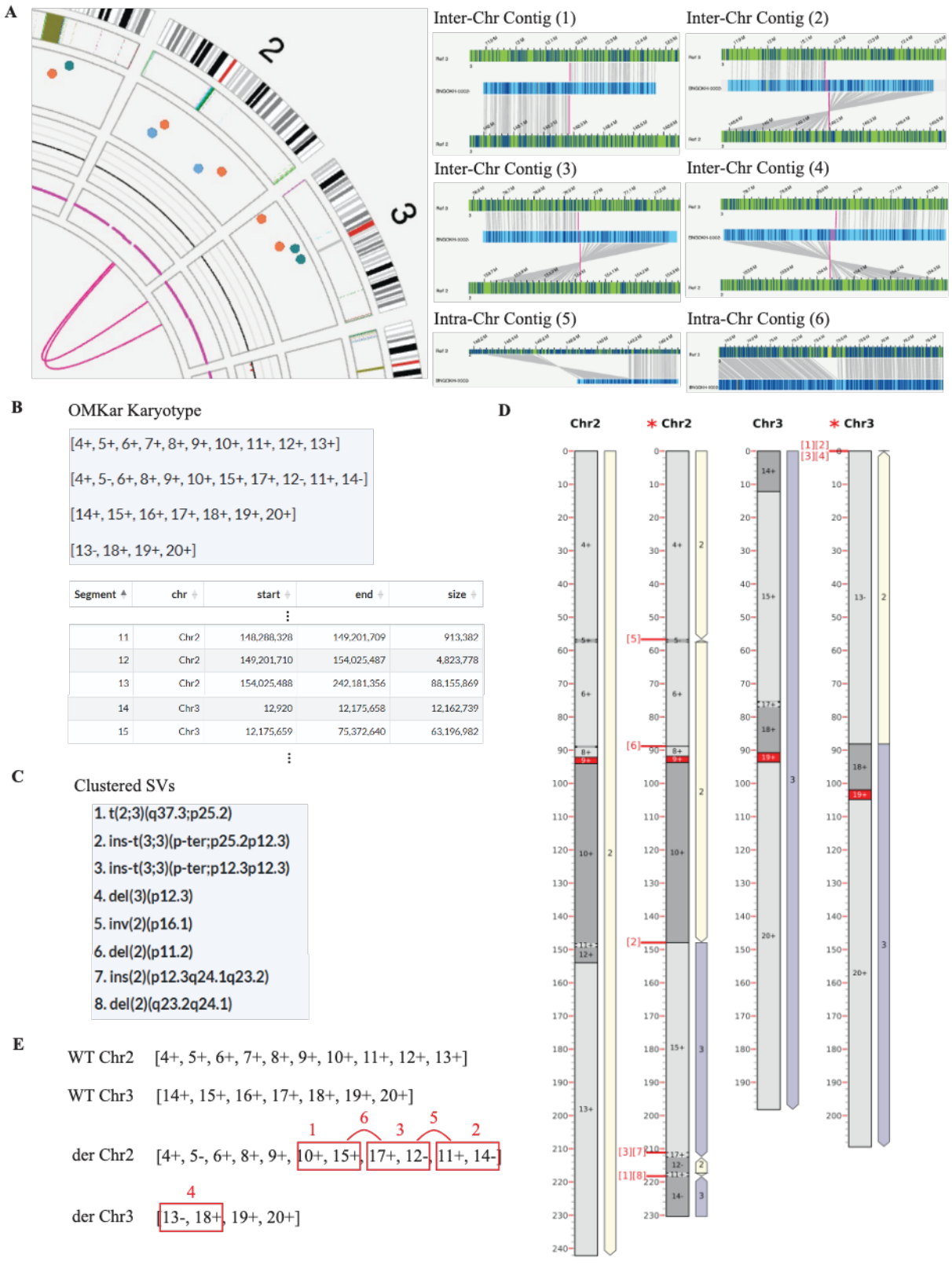

Supplementary Figure S5 caption on next page)

Supplementary Figure S5: Supplementary Figure S5: Comparison of Bionano Access and OMKar Outputs Postnatal 2281). Postnatal sample 2281 contains a set of complex translocations called between Chromosomes 2 and 3. (A) There are four translocations called but shown only as two distinct curves in the Circos plot from Bionano Access because of overlaps. The detailed contig alignments from the Genome Browser View are shown on the right. The four translocations occur at two distinct breakpoint regions, with each region involving a pair of translocations in di erent orientations. In addition, an inversion and a deletion call were also found in the region. (B) The OMKar output on the same data gives a clear description of the karyotype as a sequence of chromosomal segments (e.g., ...10+ 15+ 17+ 12-... in derivative Chromosome 2), where each segment number corresponds to a distinct genomic interval. (C) A chromosomal annotation of the OMKar reconstruction shows the complexity of this karyotype which is a non-canonical translocation event that explains all 4 translocations reported by Bionano. The derivative Chromosome 2 starts with an inversion of segment 5 and a deletion of segment 7, followed by the translocation to segment 15, a deletion of segment 16, translocation back to the reversed segment 12, an inversion to segment 11, and translocation to the inverted segment 14. The derivative Chromosome 3 is a canonical translocation of the inverted segment 13 to segment 18. (D) As part of the automated OMKar report, the clustered SVs are also shown in ISCN format. (E) The automated chromosomal ideogram corresponding to the reconstruction is included on the right, with the chromosomal segments and the location of the clustered SV labeled.

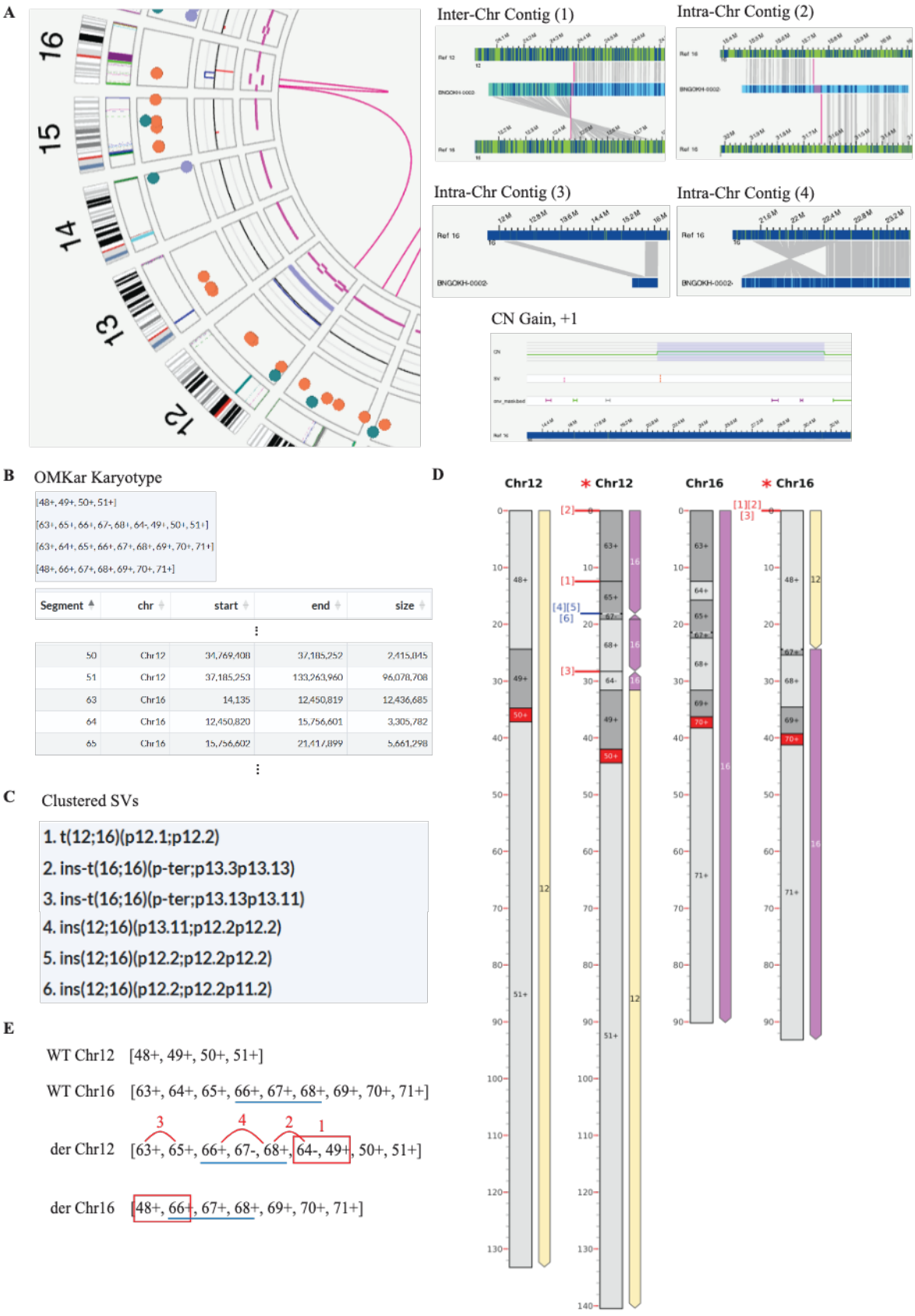

Supplementary Figure S6 caption on next page)

Supplementary Figure S6: Supplementary Figure S6: Comparison of Bionano Access and OMKar Outputs Postnatal 2282). Postnatal sample 2282 contains a set of complex translocations called between Chromosomes 12 and 16. (A) One inter-chromosomal translocation, one intra-chromosomal translocation, one deletion, one inversion, and one copy number gain were called and shown in the Circos plot from Bionano Access. The detailed contig alignments and CNV region from the Genome Browser View are shown on the right. (B) The OMKar output on the same data gives a clear description of the karyotype as a sequence of chromosomal segments. (C) A chromosomal annotation of the OMKar reconstruction shows the complexity of this karyotype which is a non-canonical translocation event that explains all SV calls from Bionano and the CNV call that was not entirely aligned with the SV calls. The derivative Chromosome 12 starts on the p-arm of Chromosome 16 with a deletion of segment 64, followed by an inversion of segment 67, the intra-chromosomal translocation to the inverted segment 64, and the inter-chromosomal translocation to Chromosome 12. The derivative Chromosome 16 starts on the p-arm of Chromosome 12 and it contains the translocation to Chromosome 16 with the amplified segments 66, 67, and 68. (D) As part of the automated OMKar report, the clustered SVs are also shown in ISCN format. (E) The automated chromosomal ideogram corresponding to the reconstruction is included on the right, with the chromosomal segments and the location of the clustered SV labeled.

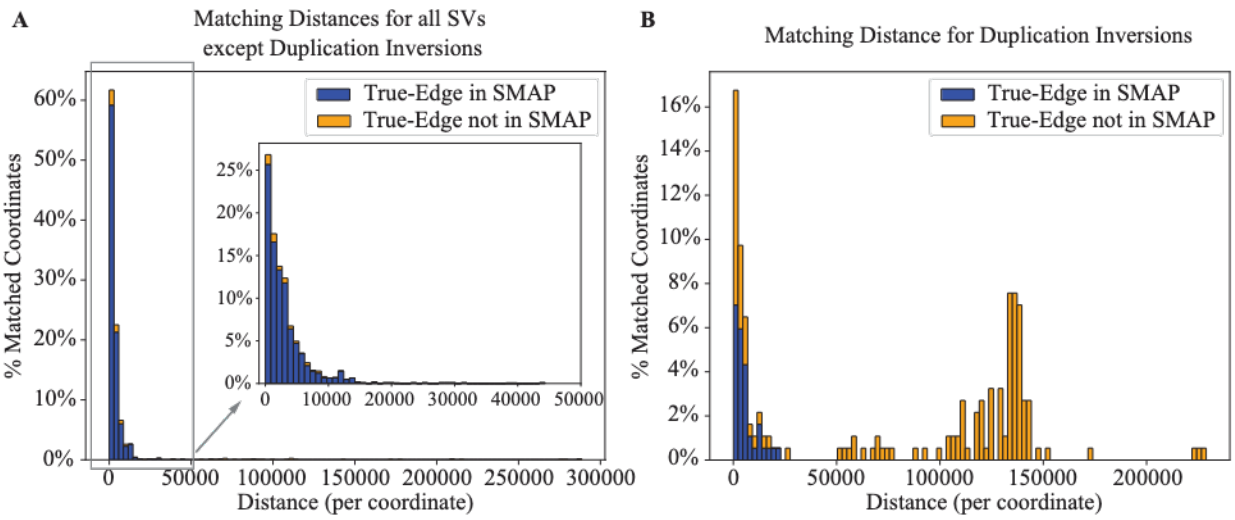

Supplementary Figure S7: Matching distances per breakpoint coordinate. The breakpoint accuracy of OMKar is analyzed by comparing OMKar reconstructions against the simulated truth karyotypes. The KarCheck SV-edge matching breakpoint distance allowance was relaxed to 300 kbp to generate these plots. For each SV, the distance for each of the two breakpoint coordinates is computed separately. For better exposition, the SVs were partitioned into A) all SVs except Duplication inversions and B) duplication inversions.

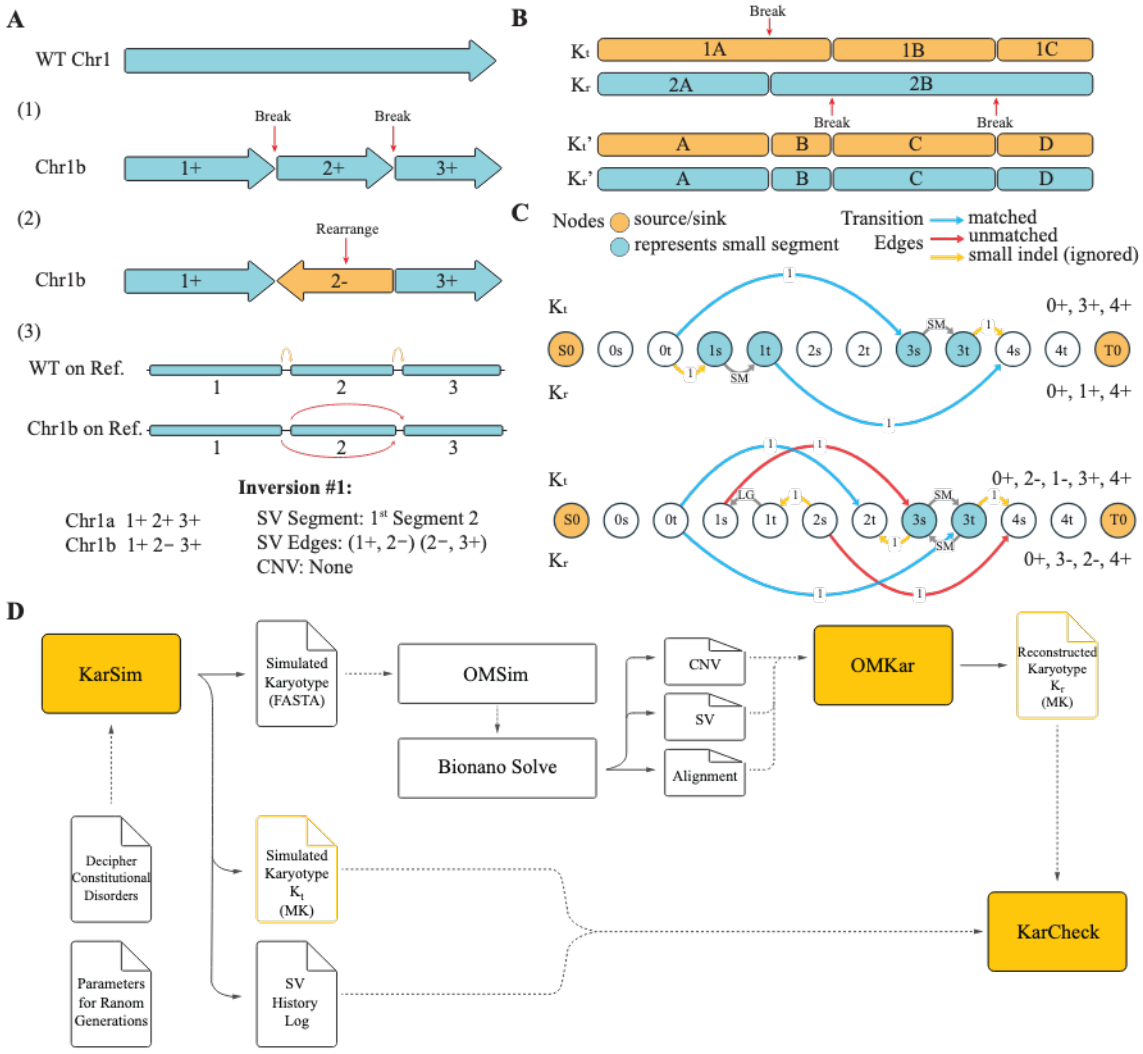

Supplementary Figure S8: KarSim and KarCheck modules. A) Implementation of the KarSim for simulating karyotypes; B) Preprocessing module of KarCheck creates matching breakpoints between two karyotypes, allowing for direct comparisons. C) KarCheck Matching. Segments are annotated by size as being SM (small) or LG (large), and D) the complete simulation and validation pipeline for OMKar.